Induction Motor Load Dynamics: Impact on Voltage Recovery Phenomena

George K. Stefopoulos, *Student Member, IEEE*, A. P. Meliopoulos, *Fellow, IEEE*

School of Electrical and Computer Engineering, Georgia Institute of Technology, Atlanta, GA 30332

***Abstract*—This paper addresses the impact of load dynamics, and in particular induction motor loads, on voltage recovery after disturbances. The paper proposes a methodology that is based on load flow techniques with advanced modeling capabilities, augmented by a simplified induction motor dynamic model. The objective is to realistically capture the dynamic characteristics of voltage recovery phenomena, avoiding, however, the full scale transient simulation. The approach uses the quadratized power flow model with explicit induction motor representation. The paper describes the modeling approach and the overall methodology for evaluating the load dynamics on voltage recovery. Preliminary results of the application of the method on a simple power system with load dynamics are also included in the paper.**

***Index Terms*— Dynamic load modeling, Induction motor model, Load flow analysis, Voltage recovery**

I. Introduction

THE paper addresses the issue of voltage recovery following a disturbance in the presence of load dynamics arising from several classes of electric loads, such as induction motors. It is well known that the voltage recovery after a disturbance in a power system is delayed by load dynamics (such as the dynamics of induction motors, etc.), especially when not enough fast reacting reactive resources (dynamic VAR sources) exist [1-9]. The phenomenon is well known to utilities and it is typically studied either using static load flow techniques or with full scale dynamic simulations. Studies are performed usually off-line, but on-line analysis is also desirable and possible.

Most off-line studies are based on traditional power flow analysis that does not take into account the dynamics of the load, while dynamic off-line studies that take into consideration the dynamics of the loads are relatively few and depend on assumed data for the dynamics of the electric load. Real time tools are almost exclusively based on traditional power flow models and they are not capable of capturing the dynamic nature of voltage recovery phenomena. This practice leads to a disconnect between system analysis and reality because the load behavior, the majority of which is electric motors, is not modeled properly.

The issue of load modeling and the effects of dynamic loads on voltage phenomena have been studied to a significant extent in literature [1-17]. In [1] the issues of voltage dips in 3-phase systems after symmetric or asymmetric faults and the accurate modeling of voltage recovery are addressed. In [2,3] the voltage recovery phenomena and the effect of induction motor loads are studied from a practical point of view, based on actual events from utility experience. References [4,5] study the voltage recovery of wind turbines after short-circuits. The issue of mitigating the delayed voltage recovery using fast VAR resources is addressed in [6-8]. The impact of induction motor loads on voltage phenomena has also been studied on a more general research basis. Reference [9] addresses the topic of voltage oscillatory instability caused by induction motors, in particular in isolated power systems, while [10] refers to the impact of induction motor loads in the system loadability margins and in the damping of inter-area oscillations. Finally, references [11-18] are indicative of current research approaches and issues in induction motor load modeling in power systems.

This paper introduces a new approach to the study of voltage recovery phenomena that can take into consideration the dynamic characteristics of the load, while avoiding the task of performing time-demanding, full-scale dynamic simulations. The approach uses load flow techniques with advanced modeling capabilities that allow a more realistic representation of load dynamics. While the methodology is capable of handling various classes of electric loads, we focus our attention to induction motor loads which represents the majority of electric loads.

The induction motor nonlinearities depend on the slip and cause singularities as the slip approaches zero. To avoid numerical problems, the proposed solution method is based on quadratization of the induction motor model. This model is interfaced with the quadratized power flow model to provide a robust solution method for a system with induction motors. In addition, this model is a more realistic representation of a power system without increasing the complexity of the power flow equations.

The paper is structured as follows: Section II elaborates on the voltage recovery problem and the issues associated with it. Section III presents a brief overview of the main features of the quadratized power flow model, along with an induction motor model for power flow studies. Section IV introduces the simplified motor dynamic model that is used in this approach and illustrates the proposed methodology for the study of voltage recovery using load flow with dynamic load

G. K. Stefopoulos and A. P. Meliopoulos are with the School of Electrical and Computer Engineering, Georgia Institute of Technology, Atlanta, GA 30332 USA (e-mail: gstefop@ieee.org, sakis.meliopoulos@ece.gatech.edu).

representation. Section V presents some preliminary results with an example test system that comprises induction motor loads. Finally, section VI concludes the paper.

II. Problem Statement

The problem of transient voltage sags during .disturbances and recovery after the disturbance has been removed is quite well known. The importance of the problem has been well identified; its significance is increasing especially in modern restructured power systems that may frequently operate close to their limits under heavy loading conditions. Furthermore, the increased number of voltage-sensitive loads and the requirements for improved power system reliability and power quality are imposing more strict criteria for the voltage recovery after severe disturbances. It is well known that slow voltage recovery phenomena have secondary effects such as operation of protective relays, electric load disruption, motor stalling, etc. Many sensitive loads may have stricter settings of protective equipment and therefore will trip faster in the presence of slow voltage recovery resulting in loss of load with severe economic consequences. A typical situation of voltage recovery following a disturbance is illustrated in Fig. 1. Note there is a fault during which the voltage collapses to a certain value. When the fault clears, the voltage recovers quickly to another level and then slowly will build up to the normal voltage. The last period of slow recovery is mostly affected by the load dynamics and especially induction motor behavior.

The objective of the paper is to present a method that can be used to study voltage recovery events after a disturbance. More specifically the problem is stated as follows: Assume a power system with dynamic loads, like, for example, induction motors. A fault occurs at some place in the system and it is cleared by the protection devices after some period of time. The objective it to study the voltage recovery after the disturbance has been cleared at the buses where dynamic or other sensitive loads are connected and also determine how these loads affect the recovery process.

This paper proposes a hybrid approach to the study of voltage recovery that is based on static load flow techniques taking also into account the essential dynamic features of the load. This approach provides a more realistic tool compared to traditional load flow, avoiding however the full scale transient simulation which requires detailed system and load dynamic models.

III. Single-Phase Quadratized Power Flow (SPQPF) with Induction Motor Representation

A. Overview of Single Phase Quadratized Power Flow

The proposed system modeling is based on the single phase quadratized power flow. The idea of this power flow model is to have a set of power flow equations of degree no greater than two, i.e. have a set of linear or quadratic equations. This can be achieved without making any sort of approximations, so the power system model is an exact model. Since most of the equations turn out to be linear and the degree of nonlinearity for the nonlinear equations is restricted to at most two, this results in improved convergence characteristics in the iterative solution and therefore improved execution speed at no expense in the accuracy of the solution.

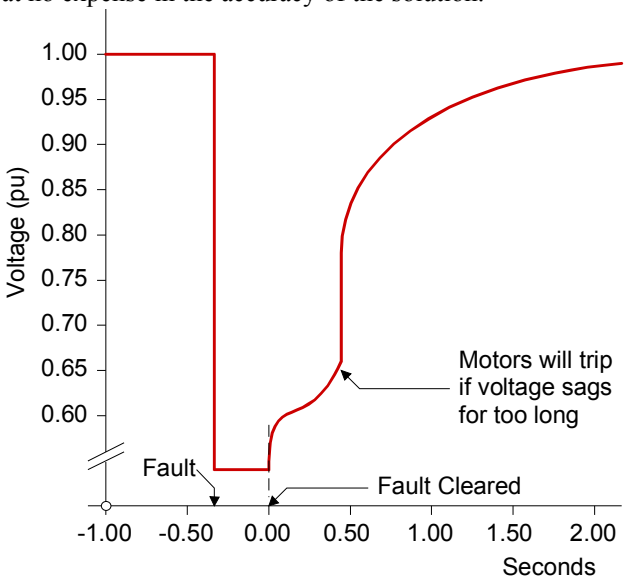

Fig. 1. Possible behavior of voltage recovery during and after a disturbance.

The first step in expressing the power flow equations in quadratic form is to avoid the trigonometric nonlinearities. This can be achieved by utilizing rectangular coordinates instead of the traditionally used polar coordinates for expressing the voltage phasors. Therefore, the system states are not the voltage magnitudes and angles, but instead the real and imaginary parts of the voltage phasors. This results in a set of polynomial equations. If the degree of nonlinearity of these equations is more than two, then quadratization of the equations can be achieved by introducing additional state variables. Note that the quadratization is performed without any approximations, and the resulting quadratic model is an exact model.

The system modeling is performed on the device level, i.e. a set of quadratic equations is used to represent the model of each device. A generalized component model is used, representing every device, which consists of the current equations of each device, which relate the current through the device to the states of the device, along with additional internal equations that model the operation of the device. The general form of the model, for any component k, is as in (1)

$$\begin{bmatrix} i^k \\ 0 \end{bmatrix} = Y^k x^k + \begin{bmatrix} x^{k^T} F_1^k x^k \\ x^{k^T} F_2^k x \\ \vdots \end{bmatrix} - b^k , \tag{1}$$

where i^k is the current through the component, x^k is the vector of the component states and b^k the driving vector for each component. Matrix Y^k models the linear part of the component and matrices F_i^k the nonlinear (quadratic) part.

Application of the connectivity constraints (Kirchoff's current law) at each bus yields the quadratized power flow equations for the whole system:

$$\begin{bmatrix} 0 \\ 0 \end{bmatrix} = Y \cdot X + \begin{bmatrix} X^T F_1 X \\ X^T F_2 X \\ \vdots \end{bmatrix} - b = G(X), \quad (2)$$

where

X : system state vector,

Y : linear term coefficient matrix (admittance matrix),

F_i : quadratic term coefficient matrix,

b : driving vector.

The solution to the quadratic equations is obtained using the Newton-Raphson iterative method:

$$X_n = X_{n-1} - J(X_{n-1})^{-1} \cdot G(X_{n-1}) \quad (3)$$

where

n : iteration step,

$J(X_{n-1})$: Jacobian matrix at iteration $n-1$.

The Iterative procedure terminates when the norm of the QPF equations is less than a defined tolerance.

Therefore, the SPQPF equations $G(X)=0$ comprise a different mathematical system of nonlinear algebraic equations compared to the traditional power flow equations. The state vector consists of the real and imaginary part of the voltage at each bus and of additional internal state variables for each device. Some of these internal states are the additional variables introduced for the quadratization of the equations. The system $G(X)=0$ consists of the current balance equations at each bus, plus additional internal equations for each one of the nonlinear devices that exist in the system. Most of the equations are linear equations. All the nonlinear equations are of order at most quadratic.

B. Induction Motor Model

Typically induction motors are represented in power system studies as constant power loads. Although this is a valid representation for steady state operation, induction motors do not always operate under constant power, especially when large deviations of voltage occur. In reality induction motors in steady state operate at a point where the electro-mechanical torque of the motor equals the mechanical torque of the electric load. As the voltage at the terminals of the induction motor changes, the operating point will change, the motor will accelerate or decelerate and during transients the operating point will not be at the intersection of the electrical torque curve and the mechanical load torque curve. We present a model here that can accommodate this behavior. The model is in quadratic form and it is integrated into the single phase quadratized power flow. In addition, the model can be used to determine the operation of the system at a specific instant of time assuming that the speed of the induction motor is fixed (for example, after a disturbance). The significance of this modeling capability is described with an example.

The importance of including the load dynamics into the power flow solution is illustrated in Figures 2 and 3. The IEEE 24-bus reliability test system (RTS) is used. Fig. 2 shows the voltage profile after a line contingency, assuming constant power load representation. Green indicates voltage magnitudes within 5% of the nominal voltage; yellow indicates a voltages deviation of more than 5%, but less than 10% of the nominal voltage; and red indicates a voltage deviation of more than 10%. Fig. 3 illustrates the same condition assuming that half of the electric load at each bus has been replaced with induction motor loads. The difference between the two figures (i.e. Figures 2 and 3) is that the induction motors in Fig. 3 operate at different slip (or speed) as dictated by the solution – at the solution the electro-magnetic torque equals the mechanical torque of the load. The reactive power absorption of the induction motors is different at different slip values and therefore they affect the voltage profile of the system. This behavior cannot be captured by a simple, static, constant power load model.

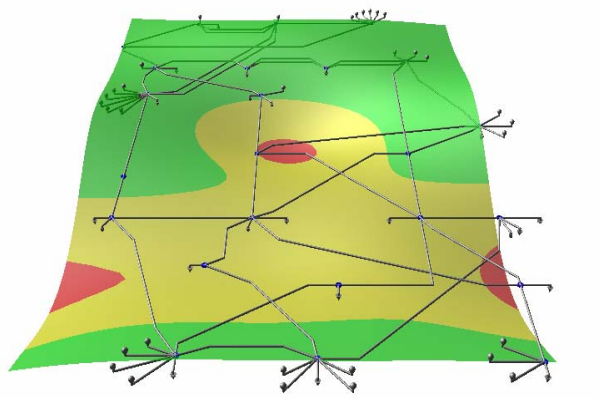

Fig. 2. Voltage profile of the 24-bus RTS after a line contingency, with constant power load representation.

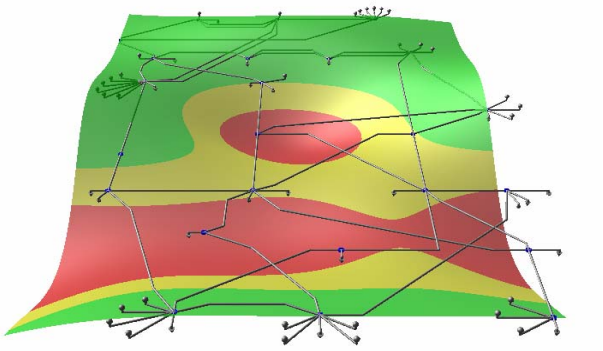

Fig. 3. Voltage profile of the 24-bus RTS after line contingency, with induction motors assuming 2% slowdown.

The induction motor model is easily included in the SPQPF formulation without increasing the degree of nonlinearity and thus further complicating the equations. A quadratic induction machine model has been developed [18] based on the typical steady state equivalent circuit of the induction motor, shown in Fig. 4. The model input data include typical motor nominal (nameplate) data, plus electrical parameters, and mechanical

load data. The model supports two mechanical loading modes: (a) Torque equilibrium (steady state), and (b) Constant Slip.

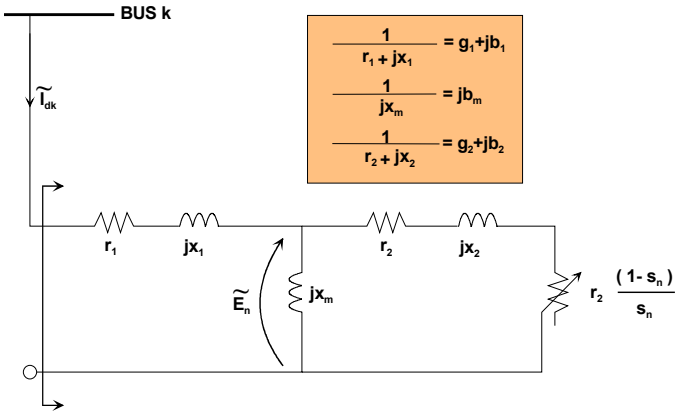

Fig. 4. Induction motor equivalent circuit.

Circuit analysis of the induction motor equivalent circuit yields the equations:

$$\begin{aligned} \tilde{I}_{dk} &= (g_1 + jb_1)(\tilde{V}_k - \tilde{E}_n) \\ 0 &= jb_m \tilde{E}_n + \tilde{E}_n \frac{s_n}{r_2 + jx_2 s_n} - (g_1 + jb_1)(\tilde{V}_k - \tilde{E}_n) \end{aligned} \tag{4}$$

An additional equation links the electrical state variables to the mechanical torque produced by the motor. This equation is derived by equating the mechanical power (torque times mechanical frequency) to the power consumed by the variable resistor in the equivalent circuit of Fig. 4.

$$T_{em}\omega_s(1 - s_n) = |I_2|^2 r_2 \frac{1 - s_n}{s_n} \tag{5}$$

or

$$0 = \left| \frac{\tilde{E}_n}{r_2 + jx_2 s_n} \right|^2 s_n r_2 - T_{em}\omega_s \tag{6}$$

where

S_n : induction motor slip,

T_{em} : mechanical torque produced by motor,

ω_s : synchronous mechanical speed.

Two compact models are defined from the above equations:

(a) Constant Slip Model (Linear):

$$\begin{aligned} \tilde{I}_{dk} &= (g_1 + jb_1)\tilde{V}_k - (g_1 + jb_1)\tilde{E}_n \\ 0 &= -(g_1 + jb_1)\tilde{V}_k + (g_1 + jb_1 + jb_m + \frac{s_n}{r_2 + jx_2 s_n})\tilde{E}_n \end{aligned} \tag{7}$$

In the constant slip mode the motor operates at constant speed. The value of the slip is known from the operating speed and therefore the model is linear. The terminal voltage $\tilde{V}_k$ and the internal rotor voltage $\tilde{E}_n$ are the states of the model. Note that the equations are given in compact complex form. In real form, separating real and imaginary parts yields a system of four linear equations. The state vector is defined as $x^T = [V_{kr} \quad V_{ki} \quad E_{ni} \quad E_{nr}]$, where the subscripts r and i denote real and imaginary parts respectively.

(b) Torque Equilibrium Model (Nonlinear):

$$\begin{aligned} \tilde{I}_{dk} &= (g_1 + jb_1)(\tilde{V}_k - \tilde{E}_n) \\ 0 &= jb_m \tilde{E}_n + \tilde{E}_n \frac{s_n}{r_2 + jx_2 s_n} - (g_1 + jb_1)(\tilde{V}_k - \tilde{E}_n) \\ 0 &= \left| \frac{\tilde{E}_n}{r_2 + jx_2 s_n} \right|^2 s_n r_2 - T_{em}\omega_s \end{aligned} \tag{8}$$

In the torque equilibrium model the slip is not constant and thus it becomes part of the state vector. Note that this model is nonlinear and not quadratic since the second and third equations contain high order expressions of state variables. In order to quadratize the model equations, we introduce three additional state variables, namely $\tilde{Y}_n$, $\tilde{W}_n$, U_n defined as follows:

$$\tilde{Y}_n = \frac{1}{r_2 + jx_2 s_n} \tag{9}$$

$$\tilde{W}_n = \tilde{Y}_n \tilde{E}_n \tag{10}$$

$$U_n = \tilde{W}_n \tilde{W}_n^* \tag{11}$$

The state vector in this mode is defined as:

$$x^T = [\tilde{V}_k \quad \tilde{E}_n \quad s_n + jU_n \quad \tilde{Y}_n \quad \tilde{W}_n].$$

The quadratic model equations are:

$$\begin{aligned} \tilde{I}_{dk} &= (g_1 + jb_1)\tilde{V}_k - (g_1 + jb_1)\tilde{E}_n \\ 0 &= -(g_1 + jb_1)\tilde{V}_k + (g_1 + j(b_1 + b_m))\tilde{E}_n + \tilde{W}_n s_n \\ 0 &= -T_{em}\omega_s + U_n s_n r_2 \\ 0 &= \tilde{W}_n \tilde{W}_n^* - U_n \\ 0 &= r_2 \tilde{Y}_n + jx_2 s_n \tilde{Y}_n - 1 \\ 0 &= \tilde{W}_n - \tilde{Y}_n \tilde{E}_n \end{aligned} \tag{12}$$

The first equation gives the stator current of the motor; the second equation comes from the equivalent circuit analysis; the third equation specifies the torque produced by the motor. The last three equations introduce the new variables for the quadratization. Note again that the state vector and the equations are given in compact complex format. They are to be expanded in real and imaginary parts to get the actual real form of the model. Note also that the third and fourth equations are real, and, therefore, the model has ten real equations and states.

The described motor model, in both operating, modes, can be immediately expressed in the generalized component form of (1) and therefore incorporated in the SPQPF formulation. The model equations are linear in the constant slip mode and

quadratic in the torque equilibrium mode, resulting in no additional complexity in the power flow equations.

After the solution of the power flow is obtained, additional internal motor quantities (rotor voltage and current, electrical torque, motor losses, etc) can be directly calculated, providing a detailed description of the motor state.

IV. Methodology For Voltage Recovery Study

The proposed approach for voltage recovery with dynamic load representation is based on appending the presented constant slip motor model with a dynamic equation describing the motor rotor dynamics. This is the rotor motion equation:

$$J \cdot \frac{d\omega_m}{dt} = T_{em} - T_L , \tag{13}$$

where

J : rotor-load moment of inertia,

ω_m : rotor mechanical speed,

T_{em} : electrical motor-torque,

T_m : mechanical load-torque.

Alternatively, this equation can be expressed in terms of the inertia constant H :

$$\frac{2H}{\omega_s} \cdot \dot{\omega}_m = T_{em} - T_L , \tag{14}$$

where

H : inertia constant (s),

ω_m : rotor mechanical speed (rad/s),

ω_s : synchronous mechanical speed (rad/s),

T_{em} : electrical torque in p.u.,

T_L : mechanical load-torque in p.u..

This simplified transient model can capture the effects of the motor in the voltage profile of the power system. The electrical transients in the motor are neglected, as they do not have significant effect in the network solution, especially for the time scales of interest, which are very long compared to the time scales of the electrical transients. Phasor representation is therefore used for the electrical quantities. The elimination of stator electrical transients makes it possible to interface the motor with the network that is assumed to operate in quasi steady state conditions.

Therefore, following a disturbance the electrical torque produced by the motor will change, due to the terminal voltage variation, causing a deviation in the torque balance between motor torque and load torque. The rotor speed will transiently change. Since there is an imbalance between the load torque and the motor torque, the rotor speed of the induction machine will change in accordance to the equation of motion.

The approach is based on solving the system of power flow equations, with the motor model at constant slip mode, along with equation (14) at discrete time steps, following the disturbance. We refer to this procedure as the time-continuation single phase quadratized power flow.

More specifically a typical scenario consists of the following phases:

1) Pre-fault phase: The system is operating at steady state condition. The solution is obtained by load-flow analysis using the motor at torque equilibrium mode.

2) During-fault phase: When a fault (or a disturbance in general) takes place the motor enters a transient operating condition. Typically, the motor is supplied by a considerably reduced voltage resulting in a decrease in the motor electro-mechanical torque. Subsequently the motor decelerates since the mechanical load will be higher than the electro-magnetic torque. Depending on the voltage level and on the mechanical load characteristics (the load may be constant torque, which is the worst case, or it may depend on the speed) the motor will decelerate and most likely will stall unless the fault is cleared and the voltage is restored in time. The deceleration of the induction motor is computed with the time-continuation single phase quandratized power flow as described earlier. Specifically at each time step the electromechanical torque and the mechanical load torque are computed and the deceleration of the motor over the time step is computed. Then the process is repeated at the new operating point. The time-continuation procedure is applied throughout the fault duration. The final operating condition at the end of the fault period provides the initial conditions for the post-fault period.

3) Post-fault phase: The time-continuation single phase quadratized power flow approach is also applied to the post-contingency system. The procedure provides the voltage recovery transient at each bus without using full-scale transient simulation during the longer post-fault period. As mentioned before, the final operating condition at the end of the fault period is the initial conditions of the post fault system.

The proposed approach is illustrated with an example test system that will help demonstrate the methodology and clarify the concepts. The example is kept relatively simple; however, the methodology is applicable to more realistic systems and scenarios, as well.

V. Preliminary Results

The proposed approach is illustrated with a simple example. The power system of Fig. 5 is assumed with induction motors connected to three buses (BUS03, BUS04, BUS05). The system consists of two generating units with their step-up transformers. The rest of the system loads, except for the motors, are constant power and constant impedance loads. The system data are given in the Appendix. A bolted three phase fault takes place in the middle of the line connecting BUS03 and BUS04. The fault is cleared after 0.2 sec by removing the faulted transmission line.

The motor mechanical loads are modeled as speed dependent loads. Their mechanical torque depends quadratically on the speed according to the (15). During the

pre-fault phase, each load torque is equal to 1 p.u.

$$T_L = a + b\omega + c\omega^2 \quad (15)$$

where

T_L : mechanical load torque (p.u.),

ω : angular velocity (p.u. of ω_s),

a, b, c : model coefficients.

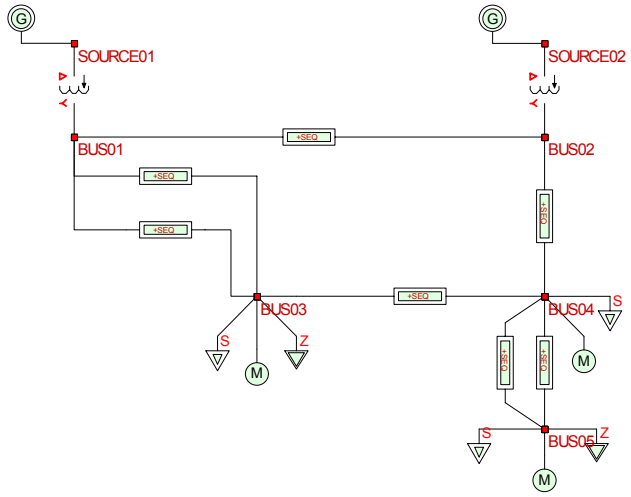

Fig. 5. Single-line diagram of the example system.

The load of motor 1, connected to BUS03, has a strong linear dependence on speed; the load of motor 2, connected to BUS04, has a strong quadratic dependence, and, finally, the mechanical load of motor 3, connected to BUS05, has a constant torque load. The mechanical load models for each motor are given in the appendix. The combined motor-load inertia constants for each motor are $H_1 = 1.5\,\text{sec}$, $H_2 = 0.5\,\text{sec}$ and $H_3 = 1.5\,\text{sec}$, for motors 1, 2 and 3 respectively.

The problem is approached based on the presented methodology. More specifically, the following phases are defined:

1) Pre-fault phase: The system is operating at steady state condition and it is easily solve by load-flow analysis. The motor is modeled at torque equilibrium mode, supplying a constant mechanical load.

2) During-fault phase: A three phase line fault takes place in the middle of the line between BUS03 and BUS04, at time t_0. The motor terminal voltage and its electrical torque are reduced due to the fault. The three motors decelerate based on (14) at a rate depending on their inertias and the terminal voltage. The fault initiation time can be assumed equal to zero without loss of generality. The fault clearing time is 0.2 sec, i.e., 12 cycles (on 60Hz period). It is important to emphasize that each motor will decelerate at different rates.

3) Post-fault phase: The fault is cleared by the removal of the faulted line. Based on the initial post-fault condition (obtained at the end of the fault period) and on the voltage recovery process the motor may reach a new steady state condition, or it may stall. During the post-fault period the analysis is again performed using the time-continuation single phase quadratized power flow. At each time step the motor accelerates based on (14), where the electrical torque produced by the motor is calculated by the solution of the power flow equations with the motor operating at constant slip mode.

Results from the test case are presented in Figures 6 through 9. Fig. 6 shows the motors speed for the three motors throughout the period of study. Note that the deceleration rate is different for each motor. Fig. 7 illustrates the voltage recovery at the motor terminal buses, for the three motors. Figures 8 and 9 present the motor active and reactive power during the pre-fault, fault and post-fault phases. Due to the different electrical and mechanical characteristics of the motors 2 and 3 compared to motor 1, and due to the system topology the recovery is considerably slower at BUS04 and BUS05, compared to BUS03.

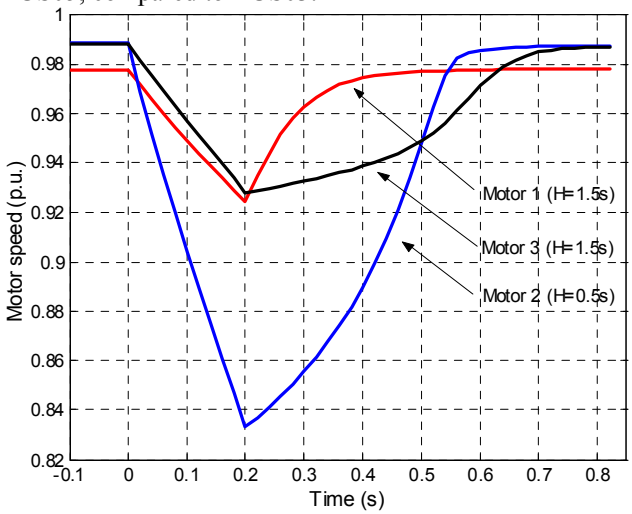

Fig. 6. Motor speed as a function of time after a 3-phase line fault.

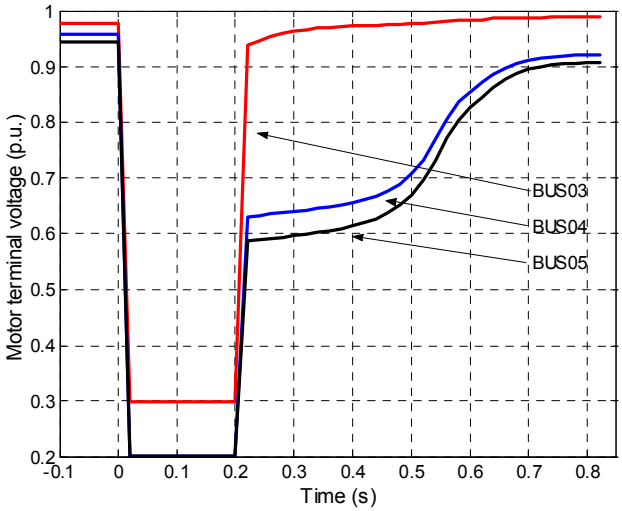

Fig. 7. Voltage recovery at motor terminal buses after a 3-phase line fault.

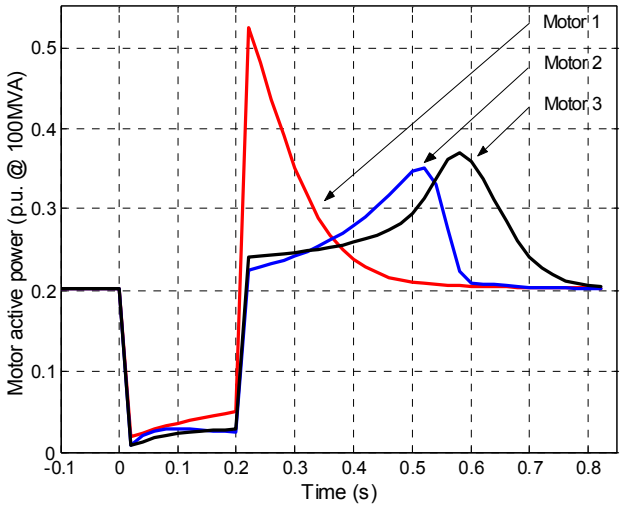

Fig. 8. Motor absorbed active power during pre-fault, fault, and post-fault periods.

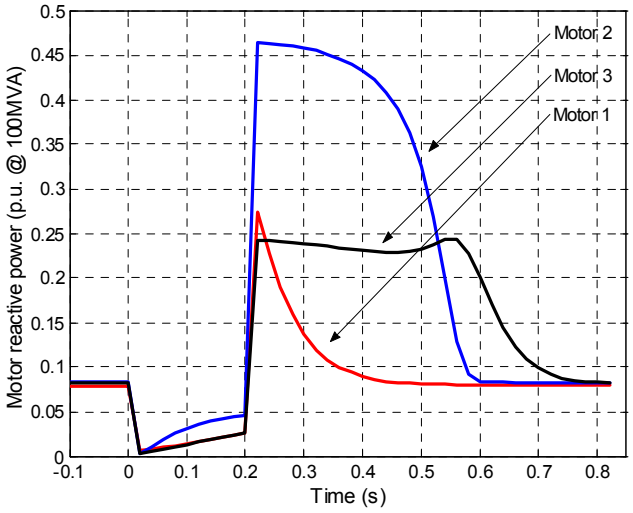

Fig. 9. Motor absorbed reactive power during pre-fault, fault, and post-fault periods.

VI. Conclusions

A practical method for realistically studying the effects of load dynamics and especially induction motor loads on voltage recovery phenomena was presented in the paper. The approach is based on load flow techniques with realistic modeling of induction motor loads. The dynamic induction motor model is solved along with the load flow equations. The single phase quadratized power flow model was used for the analysis. This method models the power system as a set of at most quadratic equations, reducing thus the degree of nonlinearity. Similarly, the induction motor loads are modeled as a set of quadratic equations that are solved simultaneously with the power flow equations. The quadratization approach provides a good approach for avoiding the stiffness of the problem when the slip approaches zero.

The trajectory of the voltage recovery (or collapse) is computed with the time-continuation single phase quadratized power flow. At each time step the motors at the various busses of the system accelerate or decelerate depending on whether the electro-mechanical torque is greater than the mechanical load torque.

The proposed methodology combines the simplicity of the standard power flow methods and the load dynamics that can be found only in full-scale time-domain simulation models. Preliminary results from several test cases on a simple power system were presented to demonstrate the process and to establish the feasibility of the approach.

VII. Appendix

The appendix contains the data of the test system.

Table I. Line Data (values at 100 MVA base)

From BUS	To BUS	Nom. V (kV)	R (p.u.)	X (p.u.)	B/2 (p.u.)
01	03	115	0.012255	0.161871	0.038661
01	03	115	0.024335	0.210308	0.030095
03	04	115	0.024335	0.210308	0.030095
02	04	115	0.024335	0.210308	0.030095
04	05	115	0.012255	0.161871	0.038661
04	05	115	0.012255	0.161871	0.038661
01	02	115	0.012255	0.161871	0.038661

Table II. Transformer Data (values at 100 MVA base)

From	To	Ratio (kV/kV)	R (p.u.)	X (p.u.)	Core conductance	Core susceptance
SOURCE 01	BUS 01	15/115	0.00467	0.05467	0.0075	0.0075
SOURCE 02	BUS 02	15/115	0.00467	0.05467	0.0075	0.0075

Table III. Induction Motor Data

Power Rating (MVA)	Nominal Voltage (kV)	Stator		Rotor		Magnetizing Reactance (p.u.)
		R (p.u.)	X (p.u.)	R (p.u.)	X (p.u.)	
20	115	0.01	0.06	0.02	0.06	3.50
20	115	0.01	0.06	0.01	0.08	3.50
20	115	0.01	0.06	0.01	0.08	3.50

Generator Data:

SOURCE01: Slack generator, Voltage 1.02 p.u.
SOURCE02: PV controlled, Volatge 1.02 p.u., P=50 MW.

Load Data:

BUS03:
Constant power: 10 MW, 7 MVAr
Constant impedance: 15 MW, 5MVAr at nominal voltage
BUS04:
Constant power: 10 MW, 3 MVAr
BUS05:
Constant power: 9 MW, 9 MVAr
Constant impedance: 15 MW, 5MVAr at nominal voltage

Mechanical Load Data:

Motor 1: $T_L = 0.1 + 0.85\omega + 0.07234\omega^2$ (p.u.)

Motor 2: $T_L = 0.05 + 0.3\omega + 0.66926\omega^2$ (p.u.)

Motor 3: $T_L = 1.0$ (p.u.)

VIII. REFERENCES

[1] M. H. J. Bollen, "Voltage recovery after unbalanced and balanced voltage dips in three-phase systems," *IEEE Trans. on Power Systems*, vol. 18, issue 4, Oct. 2003, pp. 1376-1381.

[2] B. R. Williams, W. R. Schmus and D. C. Dawson, "Transmission voltage recovery delayed by stalled air conditioner compressors," *IEEE Trans. on Power Systems*, vol. 7, no. 3, Aug. 1992, pp. 1173-1181.

[3] L. Y. Taylor, and S. -M. Hsu, "Transmission voltage recovery following a fault event in the Metro Atlanta area," *Proceedings of the 2000 IEEE-PES Summer Meeting*, July 16-20, 2000, pp. 537-542.

[4] T. Sun, Z. Chen and F. Blaabjerg, "Voltage recovery of grid-connected wind turbines after a short-circuit fault," *Proceedings of the 29th Annual Conference of the IEEE Industrial Electronics Society (IECON '03)*, vol. 3, Nov. 2-6, 2003, pp. 2723-2728.

[5] T. Sun, Z. Chen and F. Blaabjerg, "Voltage recovery of grid-connected wind turbines with DFIG after a short-circuit fault," *Proceedings of the 35th Annual IEEE Power Electronics Specialists Conference (PESC '04)*, vol. 3, June 20-25, 2004, pp. 1991-1997.

[6] L. Haijun and H. W. Renzhen, "Preventing of transient voltage instability due to induction motor loads by static condenser," *Proceedings of the 1994 IEEE Conference on Industrial Technology*, Dec. 5-9, 1994, pp. 827-831.

[7] A. E. Hammad and M. Z. El-Sadek, "Prevention of transient voltage instabilities due to induction motor loads by static VAR compensators," *IEEE Trans. on Power Systems*, vol. 4, no. 3, Aug. 1989, pp. 1182-1190.

[8] I.A. Hamzah and J. A. Yasin, "Static VAR compensators (SVC) required to solve the problem of delayed voltage recovery following faults in the power system of the Saudi electricity company, western region (SEC-WR)," *Proceedings of the 2003 IEEE PowerTech Conference*, vol. 4, Bologna, Italy, June 23-26, 2003.

[9] F. P. de Mello, and J. W. Feltes, "Voltage oscillatory instability caused by induction motor loads," *IEEE Trans. on Power Systems*, vol. 11, no. 3, Aug. 1996, pp. 1279-1285.

[10] N. Martins, S. Gomes Jr., R. M. Henriques, C. B. Gomes, A. de Andrade Barbosa, and A. C. B. Martins, "Impact of induction motor loads in system loadability margins and damping of inter-area modes," *Proceedings of the 2003 IEEE-PES General Meeting*, Toronto, Canada, July 13-17, 2003.

[11] J. Undrill, A. Renno, and G. Drobnjak, "Dynamics of a large induction motor load system," *Proceedings of the 2003 IEEE-PES General Meeting*, Toronto, Canada, July 13-17, 2003.

[12] K. Morison, H. Hamadani, and L. Wang, "Practical issues in load modeling for voltage stability studies," *Proceedings of the 2003 IEEE-PES General Meeting*, Toronto, Canada, July 13-17, 2003.

[13] K. Tomiyama, S. Ueoka, T. Takano, I. Iyoda, K. Matsuno, K. Temma, and J. J. Paserba, "Modeling of Load During and After System Faults Based on Actual Field Data," *Proceedings of the 2003 IEEE-PES General Meeting*, Toronto, Canada, July 13-17, 2003.

[14] I. R. Navarro, O. Samuelsson, and S. Lindahi, "Automatic determination of parameters in dynamic load models from normal operation data," *Proceedings of the 2003 IEEE-PES General Meeting*, Toronto, Canada, July 13-17, 2003.

[15] I. R. Navarro, O. Samuelsson, and S. Lindahi, "Influence of normalization in dynamics reactive load models," *IEEE Trans. on Power Systems*, vol. 18, issue 2, May 2003, pp. 972-973.

[16] C. –J. Lin, A. Y. –T. Chen, C. –Y. Chiou, C. –H. Huang, H. –D. Chiang, J. –C. Wang and L. Fekih-Ahmed, "Dynamic load models in power systems using the measurement approach," *IEEE Trans. on Power Systems*, vol. 8, issue 1, Feb. 1993, pp. 309-315.

[17] D. Karlsson and D. J. Hill, "Modelling and identification of nonlinear dynamic loads in power systems," *IEEE Trans. on Power Systems*, vol. 9, issue 1, Feb. 1994, pp. 157-166.

[18] A. P. Sakis Meliopoulos, Wenzhong Gao, Shengyuan Li, G. J. Cokkinides and Roger Dougal, "Quadratized induction machine model for power flow analysis," *Proceedings of the Second IASTED International Conference*, *EuroPES*, Crete, Greece, pp 194-199, June 25-28, 2002.

[19] A. P. Sakis Meliopoulos, George. J. Cokkinides and Thomas J. Overbye, "Component monitoring and dynamic loading visualization from real time power flow model data", *Proceedings of the 37st Annual Hawaii International Conference on System Sciences*, p. 58 (pp. 1-6), Big Island, Hawaii, January 5-8, 2004.